The Journal of Supercomputing
https://doi.org/10.1007/s11227-018-2608-y

Semi-real-time removal of baseline fluctuations in electrocardiogram (ECG) signals by an infinite impulse response low-pass filter (IIR-LPF)

Jeong-Hwan Kim[1] · Kang-Hwi Lee[1] · Jeong-Whan Lee[1] · Kyeong-Seop Kim[1]

Abstract

The suppression of baseline disturbance in electrocardiogram (ECG) is necessary to avoid distorting diagnostic features in the data. In order to remove baseline drift, digital filter specifications had been designing along with detrending fluctuation algorithms. However, all these methods require a high amount of off-line computation. To address this, we propose a new method to remove baseline drift in ECG signals with semi-real-time computation while compensating for the phase distortion from the frequencies in the passband of the infinite impulse response low-pass filter and estimating its sample delay for the filtered signal. Regarding evaluation of the proposed filter, we can find the fact that the signal-to-noise ratio increases by approximately 3 dB after applying the filter to the MIT-BIH stress data consisted of arrhythmias corrupted with the intentional baseline wander and the disturbances due to muscle interactions as well as electrode–skin impedance mismatch during the electrocardiogram recordings.

Keywords Baseline fluctuations · Electrocardiogram (ECG) · Infinite impulse response filter (IIR)

✉ Kyeong-Seop Kim
kyeong@kku.ac.kr

Jeong-Hwan Kim
zindevil@kku.ac.kr

Kang-Hwi Lee
kku99lkh@kku.ac.kr

Jeong-Whan Lee
jwlee95@kku.ac.kr

[1] Biomedical Engineering, School of ICT Convergence Engineering, College of Science and Technology, Konkuk University, Chungju, Korea

Published online: 17 September 2018

1 Introduction

One important aspect of a digital healthcare system involves daily heart activity monitoring in an unobtrusive manner for delivery of telecardiology health services [1]. These are based on the ambulatory electrocardiogram (ECG) signal sensed using a wearable device and transmitted via mobile devices including smartphones [2, 3]. For instance, a contactless heart rate monitoring scheme was suggested to estimate unobtrusive measures in ECG signals by establishing the strong correlations between the emotions expressed in human speech spectral features and heart rates [4]. Furthermore, the cardiac-episode diagnosis and therapy data had been accepting as the highly useful big data, and consequently, the convergence-data model was implemented by analyzing semantic relations of cardiac-episode of coronary arteriogram [5]. However, ECG data are particularly vulnerable to baseline fluctuations caused by a patient's physical movement in daily life (including respiration) or an impedance mismatch between the subject's skin and the adhesive electrodes.

The baseline drift in the ECG signal is interpreted as additive noises with frequency ranging from 0.05 to 0.5 Hz and nonstationary varying amplitude [6]. Luong, et al. [7] tried to estimate the baseline potentials by initially determining the zero-crossing points by resolving P-onset, QRS-onset/offset, and T-offset based on the first and second derivatives of an ECG segment. The baseline drift is then estimated as the third-order cubic spline interpolated on the zero crossings. Berthouze et al. [8] extended the adaptive time-varied detrending fluctuation analysis to check for the existence of a long-term temporal trend within neurophysiological signals through assessment of time-varying scaling exponents.

A hierarchical model using a blind source separation method was proposed to eliminate baseline wander in the ECG by assuming that this noise came from an independent and unknown source [9]. Agrawal et al. [10] presented a method for removing baseline wander from ECG signals by modeling the baseline drift as a first-order Brownian-motion fractal process and proposing a projection operator to separate the drift from ECG data. An adaptive filter was implemented to remove baseline distortions in ECG signals based on the constrained stability least mean square (CSLMS) algorithm which reduced the mean square error (MSE) from the least mean square (LMS) filtering process [11]. Chianca et al. [12] proposed a Fourier detrended fluctuation method in which the periodic time series was expressed as a Fourier expansion. The global trends in the data were removed by excluding the first few Fourier-coefficients and synthesizing the signal with expansions from the remnant coefficients.

A detrending method that was originally proposed for eliminating slow-varying nonstationary trends from heart rate variability (HRV) was improved to resolve the baseline drift as a global trend by merging the estimated local trends from ECG segments [13]. Wavelet transform was also considered to eliminate baseline wander in ECG data utilizing a search algorithm while computing wavelet packet coefficients [14]. Mateo, et al. [15] adopted a many adaptive linear neurons (MADLINE) neural network model to cancel baseline noise in an ECG. However, all of the previously suggested methods for the cancelation of baseline drift required a considerable amount of off-line computations and suffered from a certain amount of time delay as a result. Consequently, all these baseline-cancelation approaches are not suitable for smartphone-based healthcare applications, including the wearable heart activity monitoring system because the mobile devices used in digital healthcare systems have limited computational capacity, and the cancelation of baseline drift for mobile healthcare applications should be performed at least in semi-real time.

Digital filters were often used to suppress the unwanted signal component, i.e., noise that might distort the original strength of the sensor data. For instance, an impulse noise filter was proposed to eliminate the spurious peaks in the beacon-access points (APs) signal in real time [16]. The design specifications and computation of a finite impulse response filter (FIR) with an Android platform smartphone were attempted to eliminate the baseline wandering in the ambulatory ECG data, which was transmitted from the wearable patch-style heart activity monitoring system [17]. Although FIR filters have the advantage of unconditional stability and linear-phase response in the passband by choosing filter coefficients that are symmetrical around a center-coefficient, the filtering operation faces one main drawback: a large amount of time delay occurs getting the filtered output because the order of a FIR filter particularly designed for cancelation of baseline wander is very high due to the requirement of a narrow-stopband specification. Therefore, we suggest a new method to remove baseline wander in an ambulatory ECG signal in semi-real time by implementing the low-order Chebyshev type-II infinite impulse response low-pass filter (IIR-LPF) [18] while compensating its inherent nonlinear-phase response.

2 Removal of baseline fluctuations in an ECG by IIR filtering

Elimination of baseline drift in ECG data is essential to provide accurate data for clinical decisions involving the diagnosis of cardiac disorders, including arrhythmia. Moreover, the subtle variations in slope of the ST segment due to baseline interference may hinder the doctor from making correct decisions on especially critical conditions like myocardial infarction. To remove the interference, we may consider a FIR filter which is unconditionally stable because all of its transfer function poles are located inside the unit circle on the complex plane. Furthermore, its phase response varies linearly over the entire range of frequencies in the passband. However, concerning the removal of baseline noise, a FIR filter requires higher computational time than the equivalently constrained IIR filter because baseline interference in an ECG has a narrow spectral range. Thus, the realization of a FIR filter for the cancelation of baseline drift especially with a mobile device requires a large memory space to store filter coefficients due to its high-order realization. To cope with this problem, we primarily design an IIR filter to handle the baseline interference from ECG data because it can provide better performance than the equivalently constrained FIR filter in terms of computational time and required memory space. For our experimental simulations, the Chebyshev type-II IIR-LPF was considered because its actual frequency response optimizes its deviation from an ideal filter by incorporating maximal flat response over the passband, i.e., it keeps the absence of ripples in the passband and the equally shaped ripple attenuating response over the stopband, whereas Chebyshev type-I IIR filter contains ripples in the passband [19].

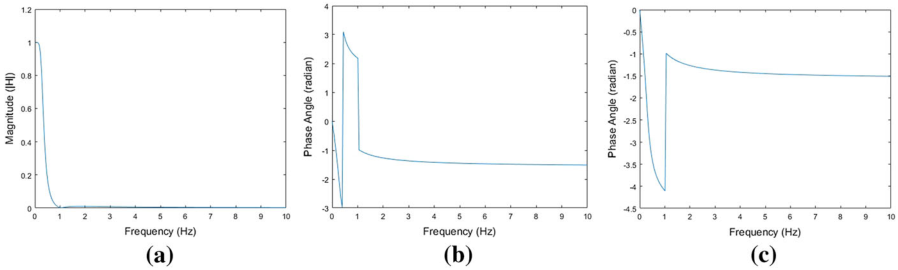

Fig. 1 Phase response of Chebyshev type-II IIR-LPF: **a** magnitude response, **b** original phase response, and **c** unwrapped phase response

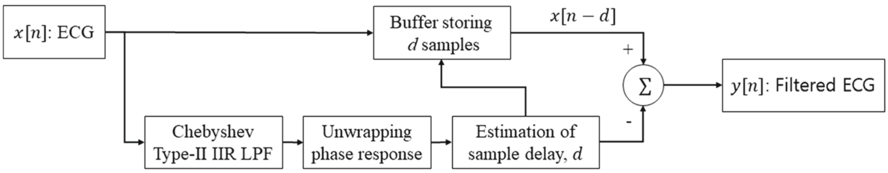

Fig. 2 Illustration of the removal of baseline fluctuations in an ECG by Chebyshev type-II IIR-LPF in semi-real-time computation

Baseline interference in ECG signals is treated as a nonstationary-global trend, and low-frequency components are extracted by a Chebyshev type-II IIR-LPF. Thus, removal of baseline drift is achieved with detrending fluctuation analysis, which involves subtracting the estimated global trend from the ECG signal. To validate our simulations, we consider the MIT-BIH arrhythmia benchmarking database [20] that consists of long-term ECG recordings obtained from real patients and digitized with a sampling rate of 360 Hz.

The main drawback of the IIR filter is that discontinuities are prone to occur in its phase response over frequencies in the passband. This discontinuity may distort morphological details of the ECG waveform, and this can lead to misdiagnosis of heart diseases. Hence, the phase angles especially in the passband must be corrected by adding or subtracting the appropriate multiples of 2π. Figure 1 shows the magnitude and the phase response of the Chebyshev type-II IIR-LPF complied to the design specifications for extracting the baseline trend with filter order, $M = 3$, sampling frequency, $f_s = 360$ Hz, passband cutoff frequency, $f_{\text{pass}} = 0.1$ Hz, and stopband cutoff frequency, $f_{\text{stop}} = 0.9$ Hz.

For the semi-real-time removal of baseline wander in an ECG, we need to estimate phase delay in terms of digital samples d by evaluating the unwrapped phase response, $\phi(f)$ as follows:

$$d = \max\left\{\frac{\phi(f)}{2\pi f} \times f_s\right\} \tag{1}$$

where f denotes frequencies over the passband and f_s is the sampling frequency (360 Hz for the MIT-BIH database). Our proposed method for removing baseline fluctuations in ECG by semi-real-time computations is illustrated in Fig. 2:

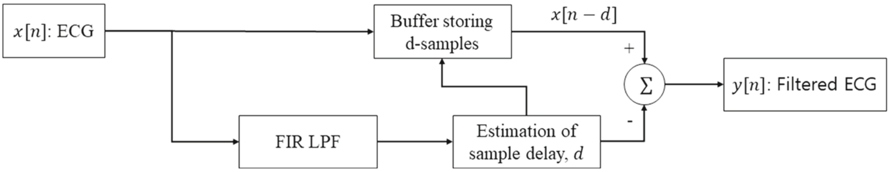

Fig. 3 Illustration of the removal of baseline fluctuations in an ECG by FIR-LPF

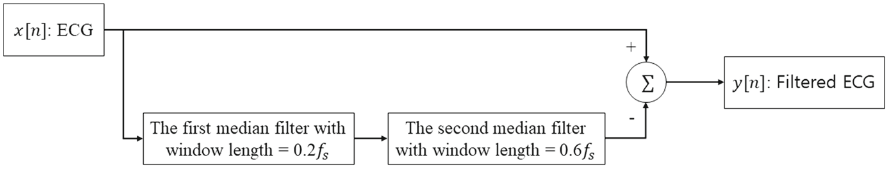

Fig. 4 Illustration of the removal of baseline fluctuations in an ECG by two cascaded median filters

In the experiments for eliminating baseline fluctuations in the ECG data, our proposed detrending method is compared with FIR filter detrending (Fig. 3) [17] and two cascaded median-filter detrending method (Fig. 4) [21] in terms of the sample delays, the size of buffer for storing input samples, the number of samples involved in filtering one output, the computational complexity and time

3 Results and discussion

To validate our proposed method, we have considered MIT-BIH record 115, for it is corrupted with real baseline fluctuations. The inherent drawback of IIR filters is that they may distort the local features of the ECG waveform due to their nonlinear-phase response. To cope with this problem, the phase angles are corrected by an unwrapping operation and the sample delays are estimated to synchronize the ECG data with the estimated baseline drift. Figure 5 demonstrates how the third-order Chebyshev type-II LPF can effectively extract the baseline wander without deforming the morphological characteristics in the original ECG data. The computational time for processing IIR filtering for 30 min-ECG data ($f_s = 360$ Hz, the total number of samples = 650,000) is 0.0156 s (AMD FX-8350 4GHz-CPU, 12GB-RAM), whereas the Parks–McClellan optimal FIR-LPF requires 0.6465 s due to its high-order design ($M = 875$) for complying with the same specifications.

Table 1 compares the results in terms of the required sample delays, the size of buffer for storing the input samples, computational complexity and time by applying median, Chebyshev II IIR-LPF and Parks–McClellan FIR-LPF detrending method, respectively.

Table 1 confirms that the computational time for eliminating baseline fluctuations with IIR-LPF detrending method was enough to be considered as a real-time computation. The computational complexity for filtering one output with median-filter detrending method can be hardly estimated due to its requirement of data sorting [22].

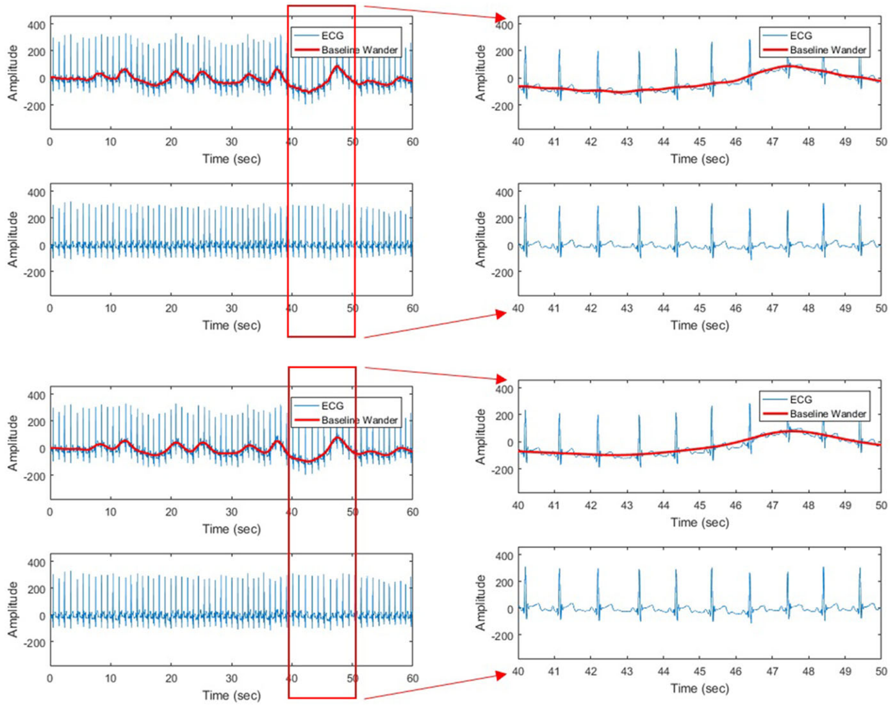

Fig. 5 Results of removing baseline fluctuations of an ECG from MIT-BIH 115 record by using Chebyshev type-II IIR-LPF: (above) $M=3, f_{\text{pass}}=0.1$ Hz, $f_{\text{stop}}=0.9$ Hz and (below) $M=3, f_{\text{pass}}=0.3$ Hz, $f_{\text{stop}}=1.7$ Hz

Table 1 Comparison of median, IIR-LPF and FIR-LPF detrending method

	Median-filter detrending	Chebyshev II IIR-LPF detrending	Parks–McClellan FIR-LPF detrending
The required sample delays for detrending (samples)	$0.6 \cdot f_s=216$	442	437
Size of buffer (samples)	$0.8 \cdot f_s=288$	442 + 3	875
Computational complexity for filtering one output (samples)	$O(N^2)$, $N=0.6 \cdot f_s+0.8 \cdot f_s$	7	875
Computational time	13.2759 s	0.0156 s	0.6465 s

The passband and stopband cutoff frequency for extracting baseline wander must be cautiously selected to avoid the morphological change especially in ST segment slope. Figure 6 presents the results from applying Chebyshev type-II IIR-LPF to 30 min-ECG data from MIT-BIH 119 database by selecting the various cutoff-frequencies of passband and stopband design specifications.

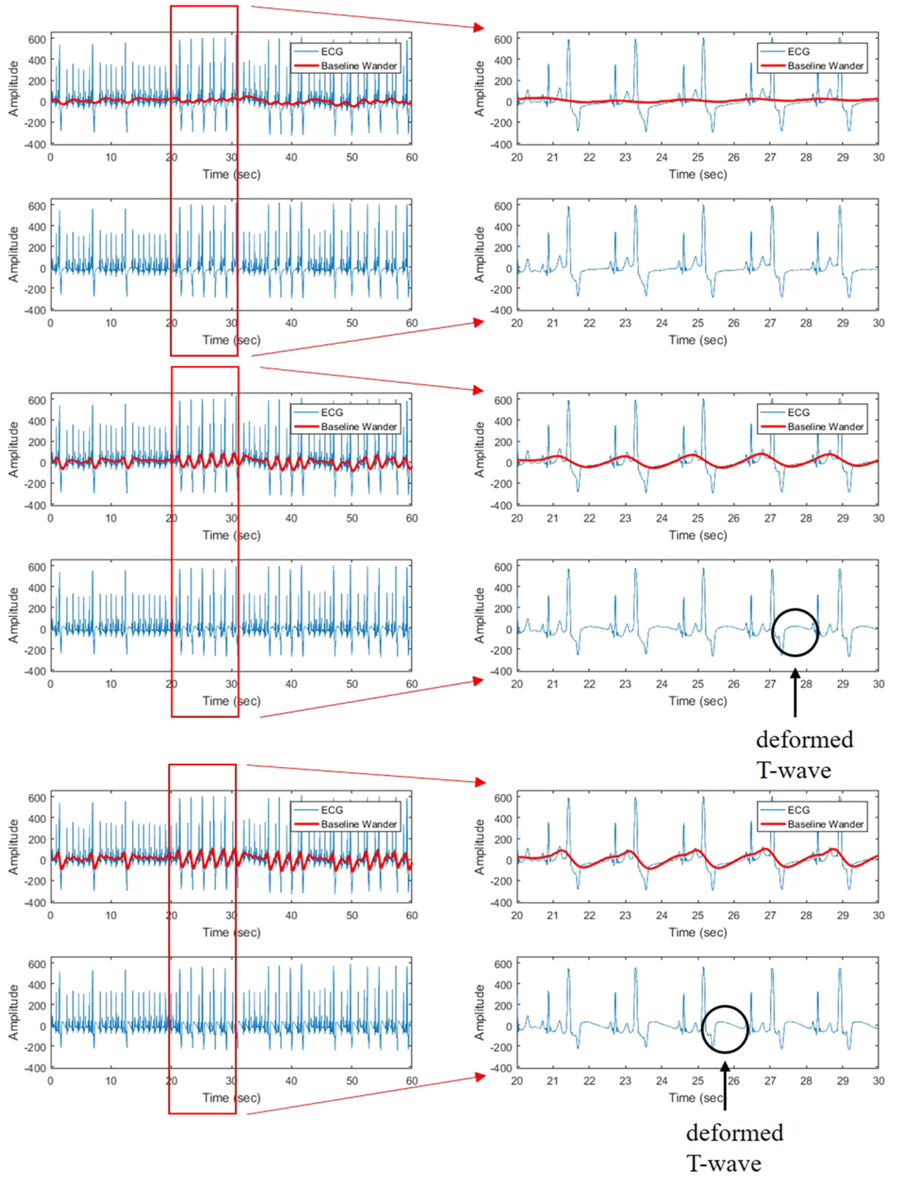

Fig. 6 Results of removing baseline fluctuations of an ECG from MIT-BIH 119 record by using Chebyshev type-II IIR-LPF: (above) $M=3, f_{\text{pass}}=0.1$ Hz, $f_{\text{stop}}=0.9$ Hz, (middle) $M=3, f_{\text{pass}}=0.3$ Hz, $f_{\text{stop}}=1.7$ Hz and (below) $M=3, f_{\text{pass}}=0.5$ Hz, $f_{\text{stop}}=2.5$ Hz

Note that the morphological shape of ECG data especially in T wave might be deformed if we select the passband cutoff frequency close to the frequency of T peak. The distorted T wave can cause the possible misleading interpretations on the slope of

Table 2 Comparison of the SNR

SNR (dB)			
MIT-BIH stress: 118		MIT-BIH stress: 119	
Original data	Filtered data	Original data	Filtered data
24	27.0409	24	27.3406
16	19.0409	16	19.3405
12	15.0410	12	15.3405
6	930,410	6	9.3406
0	3.0417	0	3.3415
− 6	− 2.9590	− 6	− 2.6595

ST segment that offers the diagnostic information about the condition of myocardial infarction.

Concerning the performance of the proposed IIR-LPF filter in terms of the signal-to-noise ratio (SNR), we have applied the filter to the MIT-BIH stress data consisted of 118 and 119 arrhythmias corrupted with the baseline wander and electromyogram (EMG) and ECG noises due to muscle interactions and the electrode–skin impedance mismatch. The considered dataset yield 24, 18, 6, 0, and − 6 dB, respectively, in SNR depends on the amount of adding noises. The SNR is estimated by

$$\mathrm{SNR}_{[\mathrm{dB}]} = 10 \times \log_{10}\left(\frac{P_{\mathrm{signal}}}{P_{\mathrm{noise}}}\right) \tag{2}$$

$$\mathrm{SNR}_{[\mathrm{dB}]} = 10 \times \log_{10}\left(\frac{\sigma^2_{\mathrm{signal}}}{\sigma^2_{\mathrm{noise}}}\right), \tag{3}$$

where P denotes the power and σ^2 is the variance.

Table 2 compares the results of applying the proposed filter to the MIT-BIH stress dataset.

Table 2 shows that the SNR can be improved by approximately 3 dB by applying the proposed filter.

4 Conclusions

In this study, the baseline fluctuations in the ECG signal are interpreted as a low-frequency global trend and resolved by a Chebyshev type-II LPF. Unlike the previously suggested detrending methods for the elimination of baseline wander, our experimental results show that the cancelation of baseline fluctuations can be performed by semi-real-time computation. Therefore, we can conclude that our proposed method can be incorporated in smartphone-based wearable heart activity monitoring systems since baseline noises can be effectively eliminated with modest computational resources.

Acknowledgements This work was supported by the National Research Foundation of Korea (NRF) grant funded by the Korean government (MSIP) (No. 2016R1A2B4016231).

References

1. Ullah F, Abdullah AH, Kaiwartya O, Kuman S, Arshad MM (2017) Medium access control (MAC) for wireless body area network (WBAN): superframe structure, multiple access technique, taxonomy, and challenges. Hum Cent Comput Inf Sci 7(34):1–39
2. Zhang Y, Liu H, Su X, Jiang P, Wei D (2015) Remote mobile health monitoring system based on smart phone and browser/server structure. J Healthc Eng 6(4):717–738
3. Kim HW, Jeong YS (2018) Secure authentication management human-centric scheme for trusting personal resource information on mobile cloud computing with blockchain. Hum Cent Comput Inf Sci 8(11):1–13
4. James AP (2015) Heart rate monitoring using human speech spectral features. Hum Cent Comput Inf Sci 5(33):1–12
5. Lee MY, Park YS, Kim MH, Lee JW (2016) A convergence data model for medical information related to acute myocardial infarction. Hum Cent Comput Inf Sci 6(15):1–15
6. Sheffield LT, Berson A, Bragg-Remschel D, Gilette PC, Hermes RE, Hinkle L, Kennedy H, Mirvis DM, Olivier C (1985) Recommendations for standard of instrumentation and practice in the use of ambulatory electrocardiography. Circulation 71(3):626A–636A
7. Luong DT, Thuan ND, Due TQ (2014) Removal of baseline noise from electrocardiography (ECG) signal based on time domain approach. Int J Biomed Sci Eng 2(2):11–16
8. Berthouze L, Farmer SE (2012) Adaptive time-varying detrended fluctuation analysis. J Neurosci Methods 209:178–188
9. Luo Y, Hargraves RH, Belle A, Bai O, Qi B, Qi X, Ward KR, Pfaffenberger MP, Najarian K (2013) A hierarchical method for removal of baseline drift from biomedical signals: application in ECG analysis. Sci World J 2013:1–10
10. Agrawal S, Gupta A (2013) Fractal and emd based removal of baseline wander and powerline interference from ECG signals. Comput Biol Med 43:1889–1899
11. Manivel K, Ravindran RS (2015) Noise removal for baseline wander and power line in electrocardiograph signals. Int J Adv Res Electr Electron Instrum Eng 4(2):1114–1122
12. Chianca CV, Ticona A, Penna TJP (2005) Fourier-detrended fluctuation analysis. Phys A 357:447–454
13. Shin SW, Kim KS, Song CG, Lee JW, Kim JH, Jeung GW (2015) Removal of baseline wandering in ECG signal by improved detrending method. Bio-med Mater Eng 26:S1087–S1093
14. Tinati MA, Mozaffary B (2006) A wavelet packets approach to electrocardiograph baseline drift cancellation. Int J Biomed Imaging 2006:1–9
15. Mateo J, Sanchez C, Vaya C, Cervigon R, Rieta JJ (2007) A new adaptive approach to remove baseline wander from ECG recordings using Madeline structure. Comput Cardiol 2007:533–536
16. Lee SG, Cha EY, Sung YS (2015) Impulse noise filter for beacon-AP signal processing in real time. J Converg 6(4):1–7
17. Kim JH, Park SE, Lee JH, Kim KS (2014) Design and implementation of digital filters for mobile healthcare applications. Int J Electron Electric Eng 2(1):75–79
18. Laghari WM, Baloch MU, Mengal MA, Shah SJ (2014) Performance analysis of analog butterworth low pass filter as compared to Chebyshev type-I filter, Chebyshev type-II filter and elliptical filter. Circuits Syst 5:209–216
19. Yadav SK, Mehra R (2014) Analysis of different IIR filter based on implementation cost performance. Int J Eng Adv Technol 3(4):267–270
20. Moody GB, Mark RG (2001) The impact of the MIT-BIH arrhythmia database: history, lessons learned, and its influence on current and future database. In: IEEE Engineering in Medicine and Biology, pp 45–50
21. Rajendra AU, Jasit SS, Jos AES, Krishnan SM (2007) Advances in cardiac signal processing. Springer, Berlin
22. Youlian Z, Cheng H (2012) An improved median filtering algorithm for image noise reduction. Phys Proc 25:609–616